

## **Supplementary Materials**

### **Unexpected ortho C-H bond activation in coordinated 7,8-benzoquinoline: Synthesis and characterisation of a heteroleptic Ir(III) 7,8-benzoquinoline complex**

Kahnu Charan Pradhan, Hemanta K. Kisan, Satyanarayan Pal\*

P. G. Dept. of Chemistry, Utkal University, Bhubaneswar, India

Email: snpal@utkaluniversity.ac.in

#### **Contents:**

1. Experimental
2. **Fig. S1:** Synthetic scheme of complex (**2**) and (**3**)
3. **Fig. S2:** IR spectrum of  $[\text{Ir}(\text{benzq})_2(\text{pyrald})]$  (**2**) in ATR mode
4. **Fig. S3:** ESI Mass spectrum of  $[\text{Ir}(\text{benzq})_2(\text{pyrald})]$  (**2**)
5. **Fig. S4:**  $^1\text{H}$  NMR spectrum of  $[\text{Ir}(\text{benzq})_2(\text{pyrald})]$  (**2**) in DMSO-d<sub>6</sub> 8.
6. **Fig. S5:** IR spectrum of  $[\text{Ir}^{\text{III}}(\text{benzq}-\kappa\text{N}, \kappa\text{C}^{10})(\text{benzq}-\kappa\text{C}^2)(\text{Hpyrald})(\text{Cl})]$  (**3**) in ATR mode
7. **Fig. S6:** ESI Mass spectrum of  $[\text{Ir}^{\text{III}}(\text{benzq}-\kappa\text{N}, \kappa\text{C}^{10})(\text{benzq}-\kappa\text{C}^2)(\text{Hpyrald})(\text{Cl})]$  (**3**)
8. **Fig. S7:**  $^1\text{H}$  NMR spectrum of  $[\text{Ir}^{\text{III}}(\text{benzq}-\kappa\text{N}, \kappa\text{C}^{10})(\text{benzq}-\kappa\text{C}^2)(\text{Hpyrald})(\text{Cl})]$  (**3**) in DMSO-d<sub>6</sub>
9. **Table S1:** Crystallographic data for complex  $[\text{Ir}(\text{benzq}-\kappa\text{N}, \kappa\text{C}^{10})(\text{benzq}-\kappa\text{C}^2)(\text{Hpyrald})(\text{Cl})]$  (**3**)
10. **Table S2:** Selected bond distances and angles of  $[\text{Ir}(\text{benzq}-\kappa\text{N}, \kappa\text{C}^{10})(\text{benzq}-\kappa\text{C}^2)(\text{Hpyrald})(\text{Cl})]$  (**3**)
11. **Fig. S8:** The hydrogen bonded dimer of  $[\text{Ir}(\text{benzq}-\kappa\text{N}, \kappa\text{C}^{10})(\text{benzq}-\kappa\text{C}^2)(\text{Hpyrald})(\text{Cl})]$  (**3**) with different types of hydrogen bonds
12. **Table: S3:** List of hydrogen bonds and C-H- $\pi$  interactions  $[\text{Ir}(\text{benzq}-\kappa\text{N}, \kappa\text{C}^{10})(\text{benzq}-\kappa\text{C}^2)(\text{Hpyrald})(\text{Cl})]$  (**3**)
13. **Fig. S9:** The  $\pi \dots \pi$  and C-H... $\pi$  interactions in  $[\text{Ir}(\text{benzq}-\kappa\text{N}, \kappa\text{C}^{10})(\text{benzq}-\kappa\text{C}^2)(\text{Hpyrald})(\text{Cl})]$  (**3**)
14. **Table: S4:** List of Intermolecular stacking parameters
15. **Fig. S10:** The packing diagram of  $[\text{Ir}(\text{benzq}-\kappa\text{N}, \kappa\text{C}^{10})(\text{benzq}-\kappa\text{C}^2)(\text{Hpyrald})(\text{Cl})]$  (**3**) is viewed perpendicular to (010) plane
16. **Fig. S11.** The Kohn–Sham orbital contours of  $[\text{Ir}(\text{benzq}-\kappa\text{N}, \kappa\text{C}^{10})(\text{benzq}-\kappa\text{C}^2)(\text{Hpyrald})(\text{Cl})]$  (**3**)
17. **Table S5:** Selected TDDFT data of  $[\text{Ir}(\text{benzq}-\kappa\text{N}, \kappa\text{C}^{10})(\text{benzq}-\kappa\text{C}^2)(\text{Hpyrald})(\text{Cl})]$  (**3**)
18. **Table S6:** Electronic, Emission and Electrochemical data of complex (**2**) and (**3**)
19. **Fig. S12:** UV-Vis spectrum of (i) complex (**2**) and (ii) complex (**3**) in dichloromethane medium
20. **Fig. S13:** Emission spectrum of (i) complex (**2**) and (ii) complex (**3**) in dichloromethane medium
21. **Fig. S14:** Cyclic voltammogram of (i) complex (**2**) and (ii) complex (**3**) in acetonitrile solution

## **1. Experimental:**

### **1.1 Materials:**

The  $\text{IrCl}_3 \cdot 3\text{H}_2\text{O}$ , pyridine-2-aldoxime, 7,8-benzoquinoline, 2-(2,4-difluorophenyl)pyridine were purchased from Sigma-Aldrich and used without further purification. All the solvents were dried by reported methods<sup>1</sup> and distilled prior to use. The dichloro bridged dimers  $[\text{Ir}(\text{benzq})_2(\mu\text{-Cl})_2\text{Ir}(\text{benzq})_2]$  and  $[\text{Ir}(\text{F}_2\text{ppy})_2(\mu\text{-Cl})_2\text{Ir}(\text{F}_2\text{ppy})_2]$  were prepared from  $\text{IrCl}_3 \cdot 3\text{H}_2\text{O}$  by 7,8-benzoquinoline (benzq) and 2(2,4-difluorophenyl)pyridine ( $\text{F}_2\text{ppy}$ ) by using the method described by Nonoyama.<sup>2</sup>

### **1.2 Physical measurement**

The infrared spectrum was recorded in ATR mode on a Thermo Scientific Nicolet iS5 FT-IR spectrophotometer. An Agilent Carry 100 UV-Vis spectrophotometer was used to collect the electronic spectra. Cyclic voltammetry measurements were performed with the help of a CH Instruments model CHI760E with acetonitrile solutions of the complexes containing  $[(n\text{-C}_4\text{H}_9)_4\text{N}]^+\text{ClO}_4^-$  (TBAP) as supporting electrolyte. The three electrode measurements were carried out at 298K under a dinitrogen atmosphere with a platinum disk working electrode, a platinum wire auxiliary electrode and a saturated calomel reference electrode (SCE). Elemental analyses were carried out on a Thermo Finnigan Flash EA1112 series elemental analyser.  $^1\text{H}$  NMR data were recorded on a Bruker 400 MHz spectrometer using  $\text{DMSO-d}_6$  as solvent. A Thermo Fisher liquid chromatograph mass spectrometer was used for determination of mass of all the complexes.

### **1.3 Crystal structure determination**

X-ray quality single crystal of  $[\text{Ir}(\text{benzq}-\kappa\text{N}, \kappa\text{C}^{10})(\text{benzq}-\kappa\text{C}^2)(\text{Hpyrald})(\text{Cl})]$  (3) was obtained from slow evaporation of dichloromethane-hexane mixture in room temperature. Data was collected on a Bruker SMART APEX CCD single crystal diffractometer, equipped with a graphite monochromator and a MoK $\alpha$  fine-focus sealed tube ( $\lambda = 0.71073 \text{ \AA}$ ) was used to determine the unit cell parameters and to collect the data at 298K. SMART software was used for data acquisition and SAINT-plus software was used for data extraction<sup>3</sup>. The absorption corrections were performed with the help of the SADABS program.<sup>4</sup> The structures were solved by direct method and refined on  $\text{F}^2$  by full matrix least-squares procedures. All the non-hydrogen atoms were refined with anisotropic thermal parameters. The hydrogen atoms were included at idealized positions using a riding model. The SHELX-97 programs<sup>5</sup> accessible in the WinGX software suite<sup>[6]</sup> were used for structure solution and refinement. The ORTEP-3 package<sup>6</sup> was used for molecular graphics. Crystallographic data was deposited with Cambridge Crystallographic Data Centre with CCDC No. 2050870 for  $[\text{Ir}(\text{benzq}-\kappa\text{N}, \kappa\text{C}^{10})(\text{benzq}-\kappa\text{C}^2)(\text{Hpyrald})(\text{Cl})]$  (3) Selected crystal and refinement data are listed in **Table S1**.

## 1.4 Computational Methods

The metal complex  $[\text{Ir}(\text{benzq}-\kappa\text{N}, \kappa\text{C}^{10})(\text{benzq}-\kappa\text{C}^2)(\text{Hpyrald})(\text{Cl})](2)$  was optimized using the Gaussian 09 Rev D.01 programme<sup>7</sup> in gas phase at the B3LYP-D3 level of theory.<sup>8</sup> The basis set used for iridium was LanL2DZ<sup>9</sup>, whereas carbons, hydrogens and nitrogens were treated with 6-31g\*\* basis set<sup>10,11</sup>. Stationary states were authenticated through Hessian indices examination. The time dependent density functional theory (TD-DFT) calculation were performed on the gas phase optimized geometry for all complexes using SMD continuum solvation model developed by Truhlar and Cramer<sup>12</sup>.

## 1.5 Synthesis of $[\text{Ir}(\text{benzq})_2(\text{pyrald})](2)$ and $[\text{Ir}(\text{benzq}-\kappa\text{N}, \kappa\text{C}^{10})(\text{benzq}-\kappa\text{C}^2)(\text{Hpyrald})(\text{Cl})](3)$

In a 100 ml round bottom flask pyridine-2-aldoxime (52 mg, 0.42 mmol) and triethylamine (0.06 ml, 0.42 mmol) were taken in 25 ml ethanol. The mixture was thoroughly mixed by stirring and added with  $[(\text{benzq})_2\text{Ir}(\mu-\text{Cl})_2\text{Ir}(\text{benzq})_2]$  (benzq=7,8 benzoquinoline) (200 mg, 0.17 mmol). The whole mixture was refluxed under N<sub>2</sub> atmosphere for 18 hours at 80°C. The reddish yellow solution thus obtained was dried under vacuum and the solid was purified on a neutral aluminium oxide column. Eluting with dichloromethane resulted a reddish yellow band as  $[\text{Ir}(\text{benzq}-\kappa\text{N}, \kappa\text{C}^{10})(\text{benzq}-\kappa\text{C}^2)(\text{Hpyrald})(\text{Cl})](3)$ . Further eluting with dichloromethane and acetone (2:1) produced an yellow coloured fraction as  $[\text{Ir}(\text{benzq})_2(\text{pyrald})](2)$ . The yields of the complexes were found to be 50 mg (21%) for (2) and 103 mg (45%) for (3) respectively. The preparation of complexes (2) and (3) also could be achieved in 2-methoxy ethanol in reflux condition.

**Selected IR bands for complex  $[\text{Ir}(\text{benzq})_2(\text{pyrald})](2)$  (ATR, cm<sup>-1</sup>)**, (Fig. S2): 1737(m), 1601(s), 1564(m), 1470(s), 1445(m), 1403(m), 1327(s), 1146(s), 1104(w), 831(s), 751(s), 718(s), 676(s), 526(m), 425(m).

**Elemental analysis:** Anal. Calcd. for C<sub>32</sub>H<sub>22</sub>ClN<sub>4</sub>OIr (2): C, 57.39; H, 3.16; N, 8.37. Found: C, 58.24; H, 3.38; N, 8.50

**ESI-MS for complex (2) (Fig. S3) :** Theoretical mass for C<sub>32</sub>H<sub>21</sub>N<sub>4</sub>OIr,  $[\text{Ir}(\text{benzq})_2(\text{pyrald})](2)$ , 670.13; Found for C<sub>32</sub>H<sub>21</sub>N<sub>4</sub>OIr,  $[\text{Ir}(\text{benzq})_2(\text{pyrald})](2)$ , 670.86.

**<sup>1</sup>H NMR for complex  $[\text{Ir}(\text{benzq})_2(\text{pyrald})](2)$  (400 MHz, DMSO-d<sub>6</sub>)**, (Fig. S4): δ 8.81 (dd, J = 5.4, 1.0 Hz, 1H), 8.54 (ddd, J = 8.0, 2.8, 1.0 Hz, 2H), 8.32 (s, 1H), 8.01 (dd, J = 5.4, 1.0 Hz, 1H), 7.96 – 7.74 (m, 5H), 7.69 (ddd, J = 10.9, 8.5, 3.4 Hz, 2H), 7.50 (d, J = 8.1 Hz, 1H), 7.45 (d, J = 7.7 Hz, 1H), 7.41 – 7.30 (m, 2H), 7.10 (t, J = 7.5 Hz, 1H), 6.98 (t, J = 7.5 Hz, 1H), 6.89 (t, J = 6.5 Hz, 1H), 6.22 (d, J = 6.9 Hz, 1H), 6.05 (d, J = 7.0 Hz, 1H).

**Selected IR bands for complex (3) (ATR, cm<sup>-1</sup>)** (Fig. S5): 1603(s), 1497(s), 1470(s), 1422(w), 1327(s), 127(w), 1125(s), 1084(w), 835(s), 752(s), 720(s), 676(s), 611(s), 562(s), 478(s), 434(s).

**Elemental analysis:** Anal. Calcd. for  $C_{32}H_{22}ClN_4OIr$  (**3**): C, 54.42; H, 3.14; N, 7.93. Found: C, 54.96; H, 3.20; N, 8.06

**ESI-MS for complex (**3**) (Fig. S6):** Theoretical mass for  $C_{32}H_{22}N_4OClIr$ ,  $[Ir^{III}(\text{benzq}-\kappa N, \kappa C^{10})(\text{benzq}-\kappa C^2)(\text{Hpyrald})(\text{Cl})]$  (**3**), 706.11; Found for  $C_{32}H_{22}N_4OClIr$ ,  $[Ir^{III}(\text{benzq}-\kappa N, \kappa C^{10})(\text{benzq}-\kappa C^2)(\text{Hpyrald})(\text{Cl})]$  (**3**), 706.83.

**$^1H$  NMR for complex (**3**) (400 MHz, DMSO-d<sub>6</sub>), (Fig. S7):**  $\delta$  9.66 (d,  $J = 8.5$  Hz, 1H), 8.99 (s, 1H), 8.64 (d,  $J = 5.3$  Hz, 1H), 8.53 (s, 1H), 8.26 (d,  $J = 8.0$  Hz, 1H), 8.14 (d,  $J = 8.1$  Hz, 1H), 8.03 (t,  $J = 8.1$  Hz, 2H), 7.90 (dd,  $J = 14.0, 8.3$  Hz, 4H), 7.73 (dt,  $J = 16.9, 8.7$  Hz, 5H), 7.50 – 7.36 (m, 1H), 7.31 (d,  $J = 5.5$  Hz, 1H), 7.02 (d,  $J = 8.6$  Hz, 1H), 6.94 (t,  $J = 6.1$  Hz, 1H).

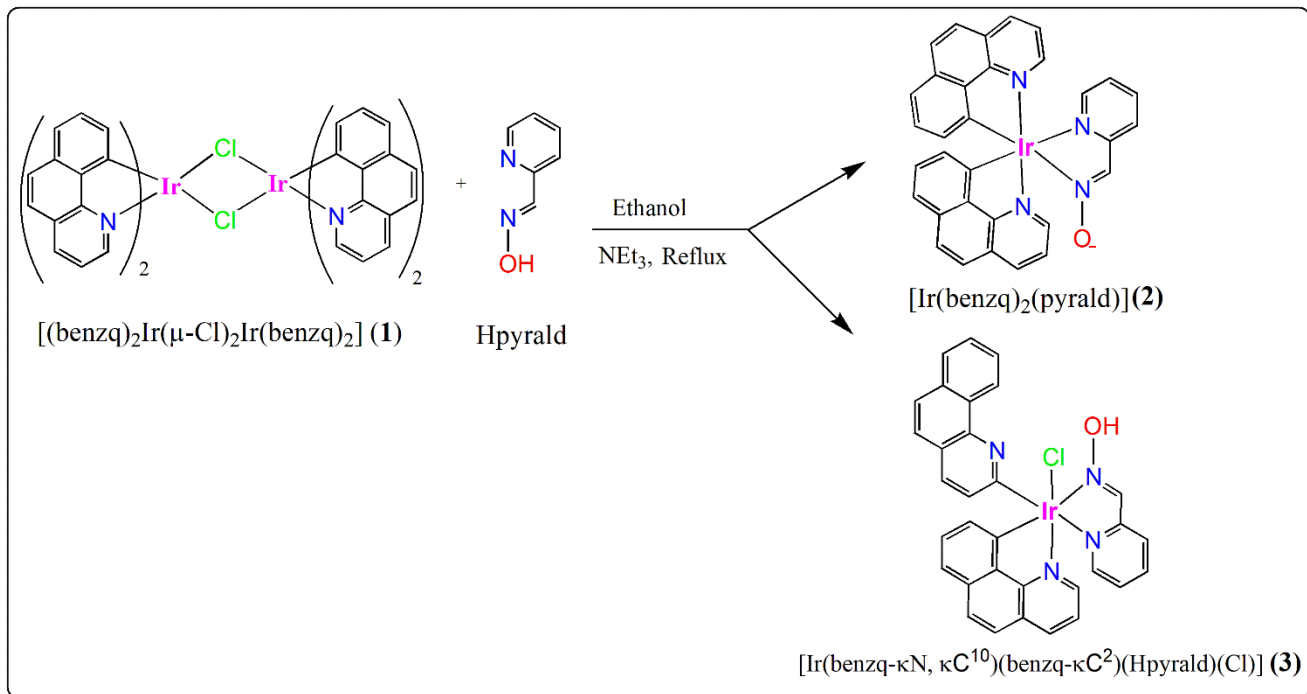


**Fig. S1:** Synthetic scheme of complex (**2**) and (**3**)

## References:

1. “Purification of Laboratory Chemicals” by W.L.F. Armarego and C. L. L. Chai, Seventh Ed., Butterworth-Heinemann (Elsevier), 2013
2. M. Nonoyama, *Bull. Chem. Soc. Jpn.* 1974, **47**, 767–768, <https://doi.org/10.1246/bcsj.47.767>.
3. SMART Version 5.630 and SAINT-plus Version 6.45, Bruker-Nonius Analytical X-ray Systems Inc., Madison, WI, USA, 2003.

4. G.M. Sheldrick, SADABS, Program for Area Detector Absorption Correction, University of Göttingen, Göttingen, Germany, **1997**.
5. G.M. Sheldrick, SHEXL-97, Structure Determination Software, University of Göttingen, Göttingen, Germany, **1997**.
6. L.J. Farrugia, WinGX and ORTEP for Windows: an update, *J. Appl. Crystallogr.* 2012, **45**, 849-854, DOI: <https://doi.org/10.1107/S0021889812029111>
7. M. J. Frisch, G. W. Trucks, H. B. Schlegel, G. E. Scuseria, M. A. Robb, J. R. Cheeseman, G. Scalmani, V. Barone, B. Mennucci, G. A. Petersson, H. Nakatsuji, M. Caricato, X. Li, H. P. Hratchian, A.F. Izmaylov, J. Bloino, G. Zheng, J. L. Sonnenberg, H. Hada, M. Ehara, K. Toyota, R. Fukuda, J. Hasegawa, M. Ishida, T. Nakajima, Y. Honda, O. Kitao, H. Nakai, T. Vreven, J. A. Jr. Montgomery, J. E. Peralta, F. Ogliaro, M. Bearpark, J. J. Heyd, E. Brothers, K. N. Kudin, V. N. Staroverov, R. Kobayashi, J. Normand, K. Raghavachari, A. Rendell, J. C. Burant, S. S. Iyengar, J. Tomasi, M. Cossi, N. Rega, N. J. Millam, M. Klene, J. E. Knox, J. B. Cross, V. Bakken, C. Adamo, J. Jaramillo, R. Gomperts, R. E. Stratmann, O. Yazyev, A. J. Austin, R. Cammi, C. Pomelli, J. W. Ochterski, R. L. Martin, K. Morokuma, V. G. Zakrzewski, G. A. Voth, P. Salvador, J. J. Dannenberg, S. Dapprich, A. D. Daniels, O. Farkas, J. B. Foresman, J.V. Ortiz, J. Cioslowski, D. J. Fox, Gaussian, Inc., Wallingford CT, **2013**.
8. S. Grimme, J. Antony, S. Ehrlich, and H. Krieg, *J. Chem. Phys.* 2010, **132**, 154104, doi.org/10.1063/1.3382344.
9. P. J. Hay, and W.R. Wadt, *J. Chem. Phys.* 1985, **82**, 299-310, doi: 10.1063/1.448975.
10. W. J. Hehre, R. Ditchfield, J. A. Pople, *J. Chem. Phys.* 1972, **56**, 2257-2261, doi: 10.1063/1.1677527.
11. P. C. Hariharan, J. A. Pople, *Theor. Chim. Acta*. 1973, **28**, 213-222, doi.org/10.1007/BF00533485
12. A. V. Marenich, C. J. Cramer, D. G. Truhlar, *J. Phys. Chem. B*, 2009, **113**, 6378, doi.org/10.1021/jp810292n

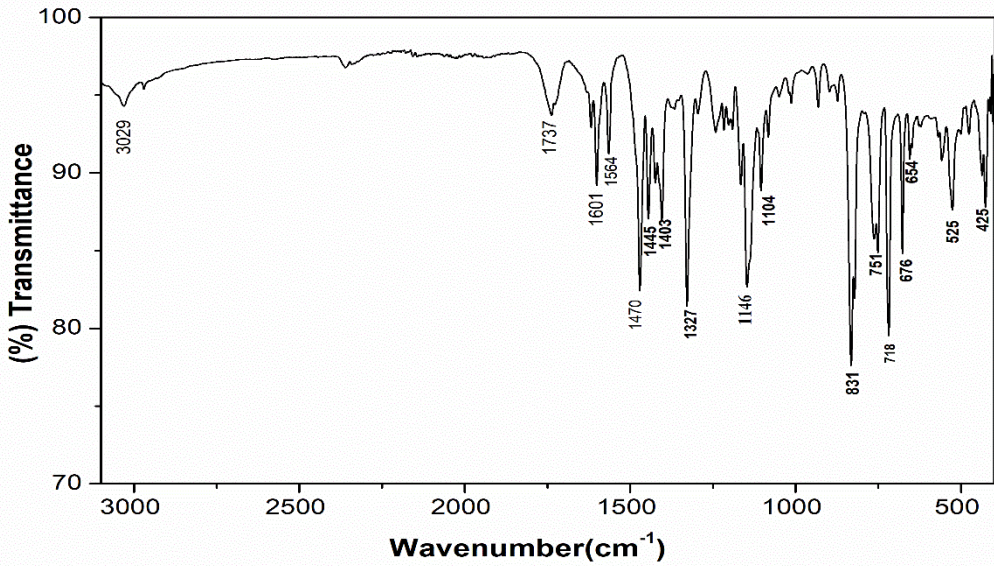


**Fig. S2:** IR spectrum of  $[\text{Ir}(\text{benzq})_2(\text{pyrald})]$  (**2**) in ATR mode

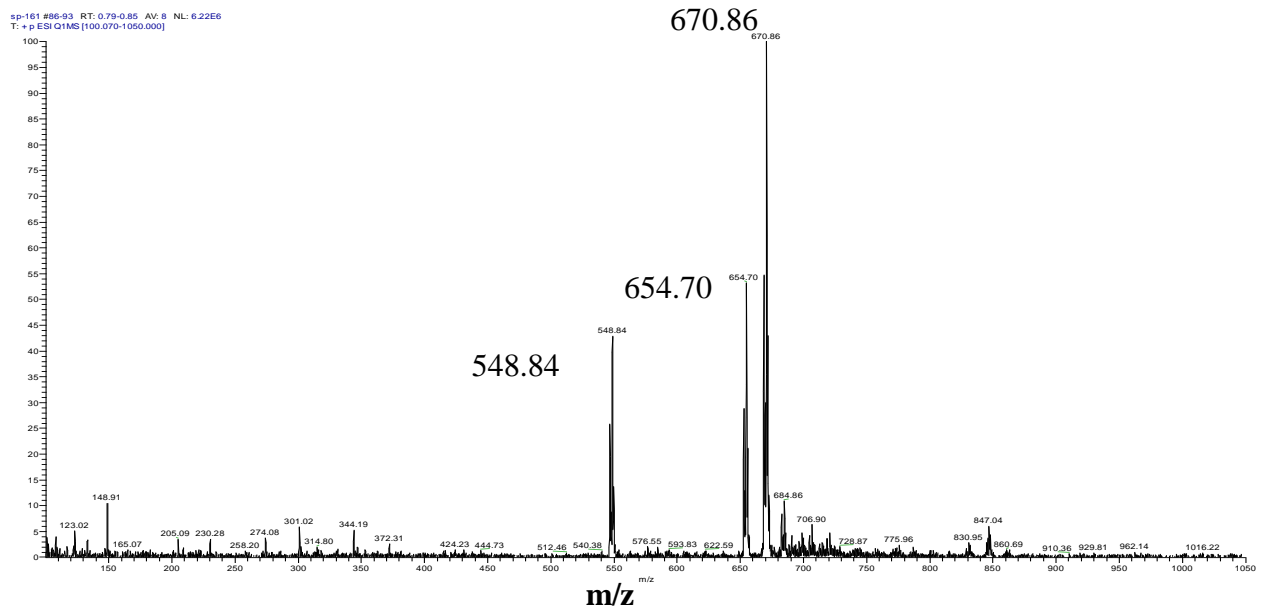


**Fig. S3:** ESI Mass spectrum of  $[\text{Ir}(\text{benzq})_2(\text{pyrald})]$  (**2**)

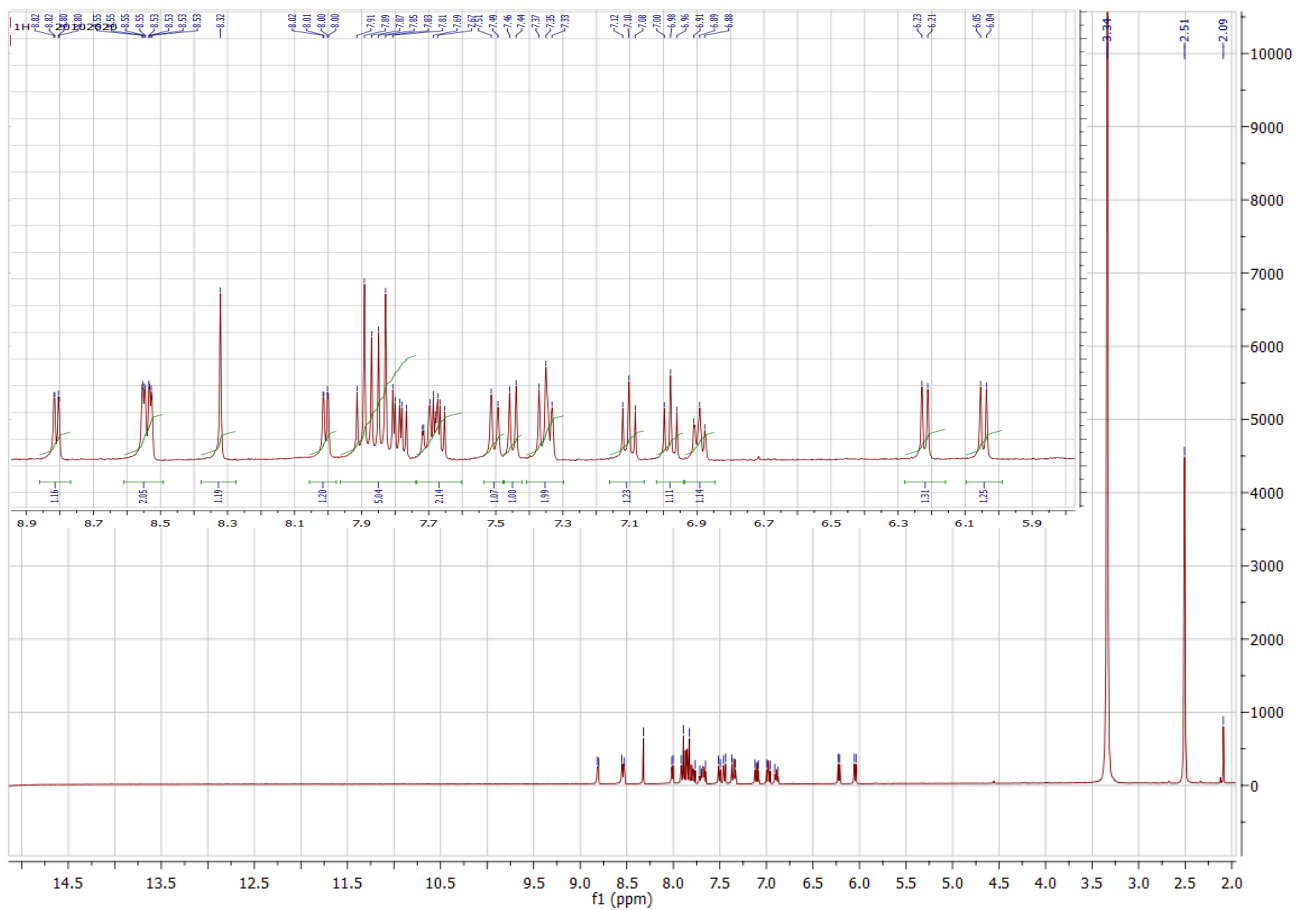


**Fig. S4:**  $^1\text{H}$  NMR spectrum of  $[\text{Ir}(\text{benzq})_2(\text{pyrald})]$  (**2**) in  $\text{DMSO-d}_6$  along with the enlarged part of 5.9 to 8.9 ppm

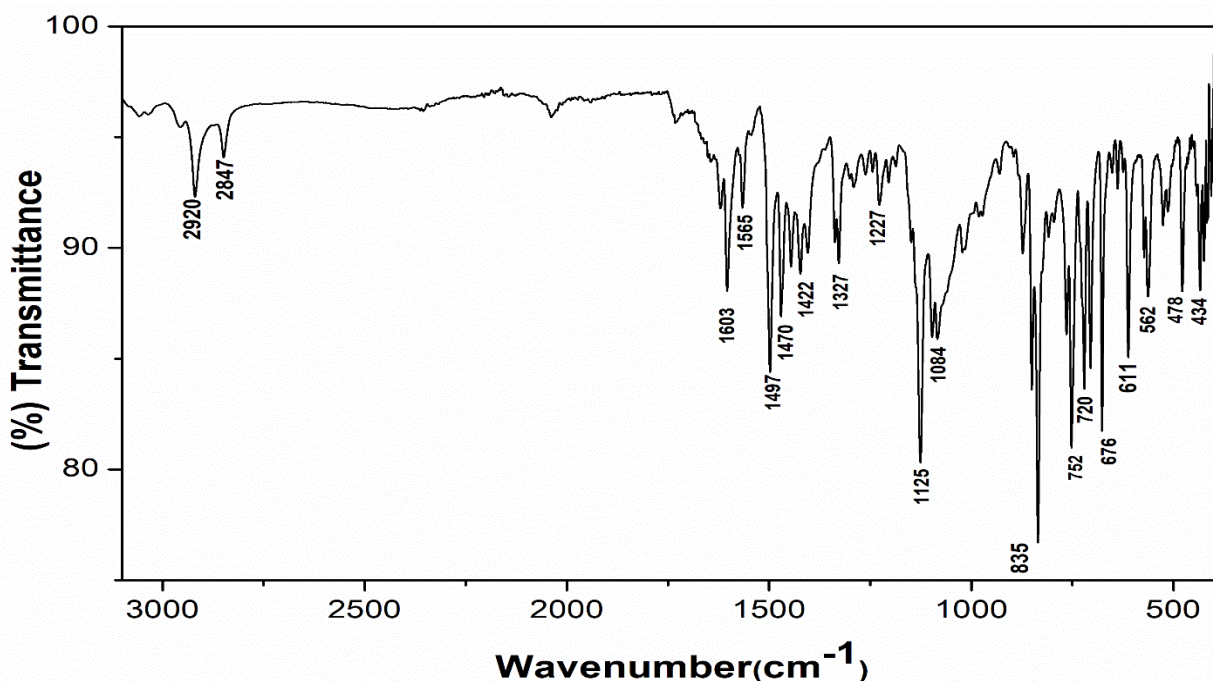


**Fig. S5:** IR spectrum of  $[\text{Ir}(\text{benzq}-\kappa\text{N}, \kappa\text{C}^{10})(\text{benzq}-\kappa\text{C}^2)(\text{Hpyrald})(\text{Cl})]$  (**3**) in ATR mode

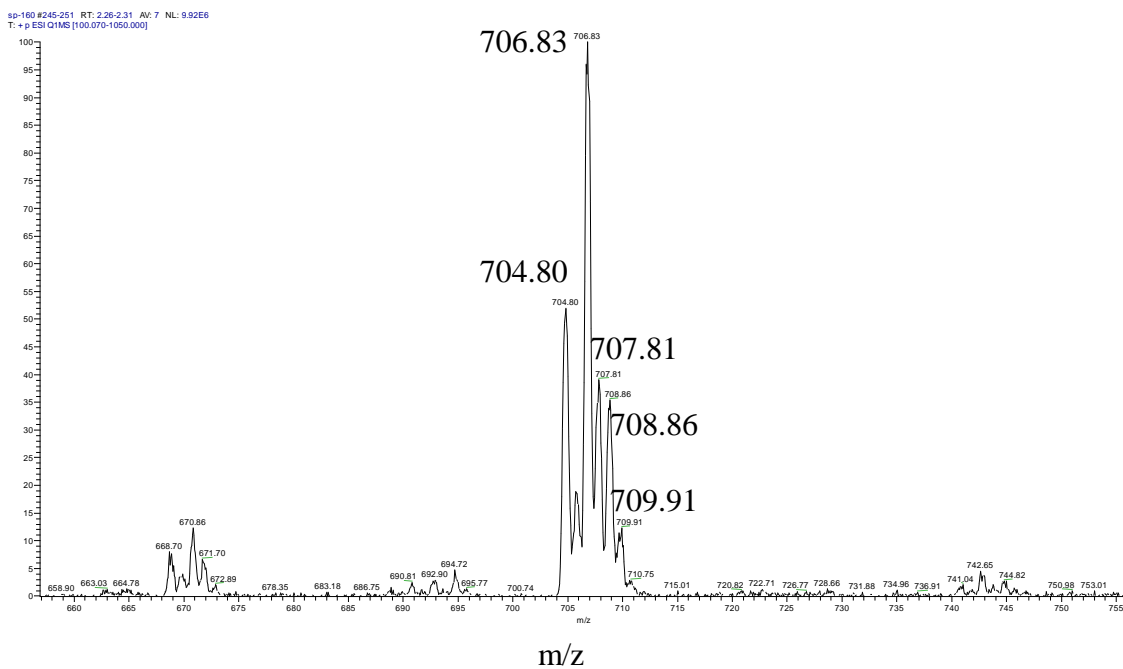


**Fig. S6:** ESI Mass spectrum of [Ir(benzq- $\kappa$ N,  $\kappa$ C<sup>10</sup>)(benzq- $\kappa$ C<sup>2</sup>)(Hpyrald)(Cl)] (3)

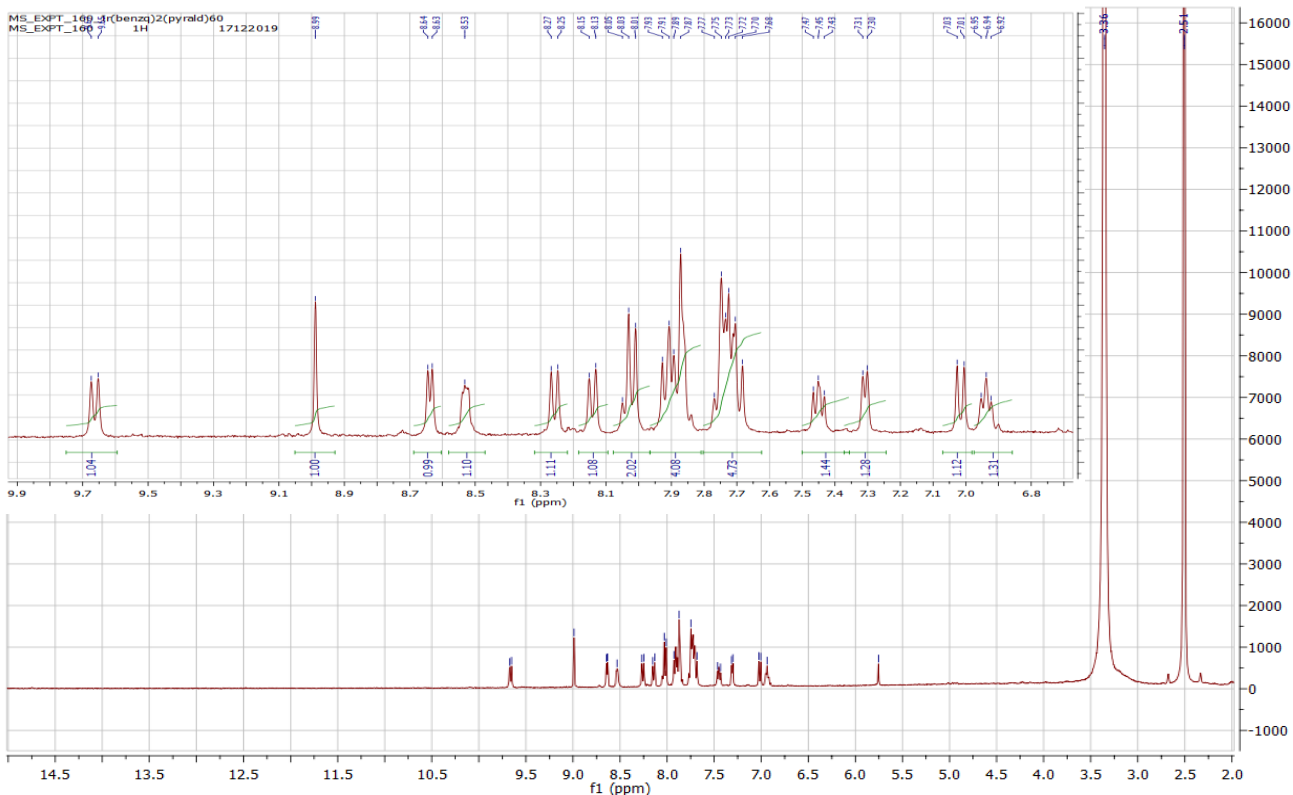


**Fig. S7:**  $^1\text{H}$  NMR spectrum of  $[\text{Ir}(\text{benzq-}\kappa\text{N}, \kappa\text{C}^{10})(\text{benzq-}\kappa\text{C}^2)(\text{Hpyrald})(\text{Cl})]$  (**3**) in  $\text{DMSO-d}_6$  along with the enlarged part of 6.6 to 9.9 ppm

**Table S1:** Crystallographic data for complex [Ir(benzq-  $\kappa$ N,  $\kappa$ C<sup>10</sup>)(benzq- $\kappa$ C<sup>2</sup>)(Hpyrald)(Cl)] (**3**)

	[Ir(benzq- $\kappa$ N, $\kappa$ C <sup>10</sup> )(benzq- $\kappa$ C <sup>2</sup> )(Hpyrald)(Cl)] ( <b>3</b> )
Empirical formula	C <sub>32</sub> H <sub>22</sub> ClIrN <sub>4</sub> O
Formula wt	706.21
Crystal system	Monoclinic
Space group	P2 <sub>1</sub> /n
a (Å)	9.2148(14)
b (Å)	28.241(5)
c (Å)	10.6998(14)
$\alpha$ (°)	90.0
$\beta$ (°)	109.745(4)
$\gamma$ (°)	90.0
V(Å <sup>3</sup> )	2620.8(7)
Z	4
$\rho$ (Mg m <sup>-3</sup> )	1.790
$\mu$ (mm <sup>-1</sup> )	5.231
Reflection collected	78829
Reflection unique	5389
Parameters	352
R1 (obs)	0.0336
wR2	0.0551
GOF	1.026
Largest peak	1.00
Deepest Hole	-0.7780

**Table S2:** Selected bond distances and angles of  $[\text{Ir}(\text{benzq}-\kappa\text{N}, \kappa\text{C}^{10})(\text{benzq}-\kappa\text{C}^2)(\text{Hpyrald})(\text{Cl})]$  (3)

Bond length (Å)			
Ir(1)-Cl(1)	2.3683(12)	Ir(1)-N(4)	2.118(4)
Ir(1)-N(1)	2.043(3)	Ir(1)-C(14)	2.023(5)
Ir(1)-N(3)	2.124(4)	Ir(1)-C(11)	2.031(5)
Bond angles (°)			
C(14)-Ir(1)-C(11)	90.72(19)	C(11)-Ir(1)-N(4)	171.72(16)
C(14)-Ir(1)-N(4)	96.09(18)	N(1)-Ir(1)-N(4)	93.69(14)
C(14)-Ir(1)-N(3)	173.36(19)	N(1)-Ir(1)-Cl(1)	173.44(10)
C(11)-Ir(1)-N(3)	95.63(18)	N(4)-Ir(1)-N(3)	77.42(16)

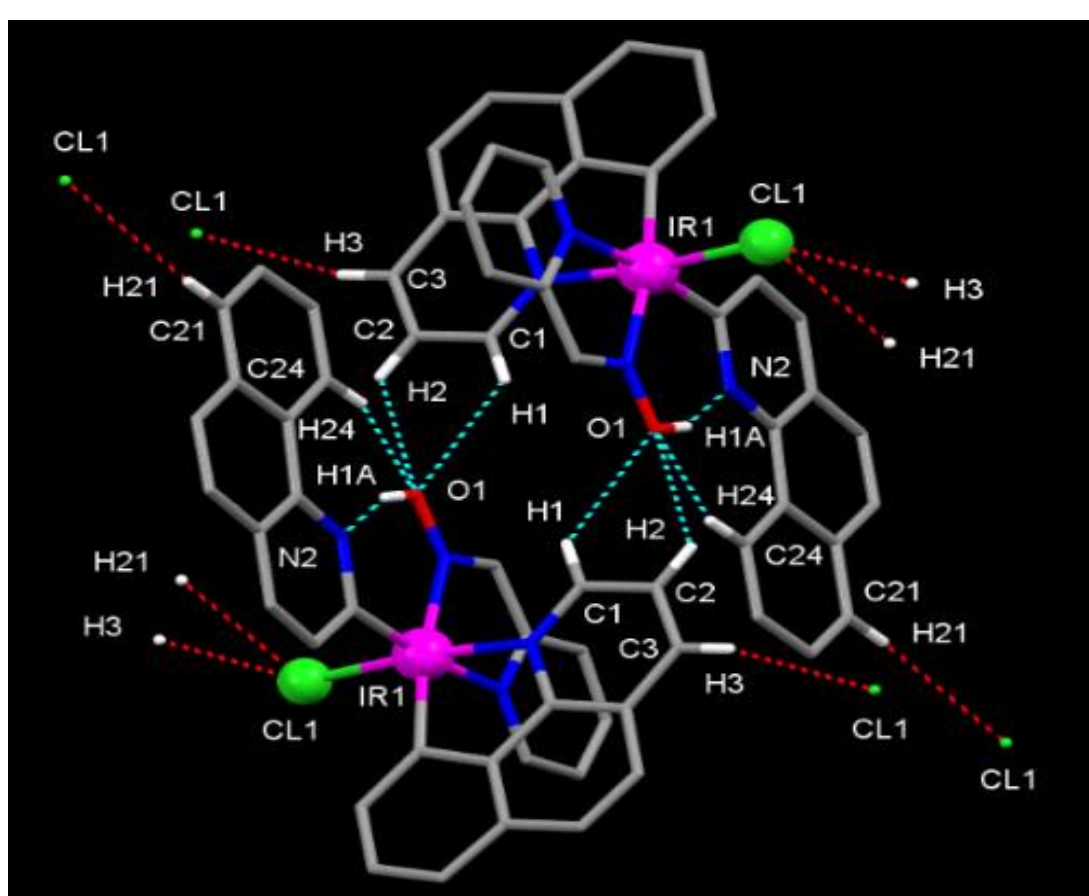
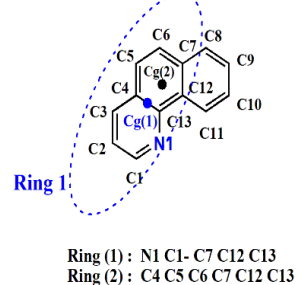


**Fig. S8:** The hydrogen bonded dimer of  $[\text{Ir}(\text{benzq}-\kappa\text{N}, \kappa\text{C}^{10})(\text{benzq}-\kappa\text{C}^2)(\text{Hpyrald})(\text{Cl})]$  (3) with different types of hydrogen bonds.

**Table: S3:** List of hydrogen bonds and C-H- $\pi$  interactions in  $[\text{Ir}(\text{benzq}-\kappa\text{N}, \kappa\text{C}^{10})(\text{benzq}-\kappa\text{C}^2)(\text{Hpyrald})(\text{Cl})] (\mathbf{3})$

D-H....A	D-H (Å)	H.....A (Å)	D.....A (Å)	D-H....A (°)
O1-H1A...N2	0.82	1.84	2.609(5)	157
C24-H24...O1	0.93	2.32	3.221(7)	160
C1-H1....O1 <sup>i</sup>	0.93	2.56	3.204(6)	127
C2-H2....O2 <sup>i</sup>	0.93	2.675	3.259	121.45
C3-H3....Cl1 <sup>ii</sup>	0.93	2.77	3.677(5)	165
C21-H21...Cl1 <sup>iii</sup>	0.93	2.78	3.647(8)	155
C29-H29...Cg1 <sup>iv</sup>	0.93	2.59	3.507(3)	168
C29-H29...Cg2 <sup>iv</sup>	0.93	2.65	3.493(8)	151



Symmetry codes: (i) 1-x, -y, -z (ii) x, y, 1+z (iii) 2-x, -y, 1-z (iv) -1+x, y, z

$Cg1 = N1/C1-C7, C12, C13$   $Cg2 = C4-C7, C12, C13$

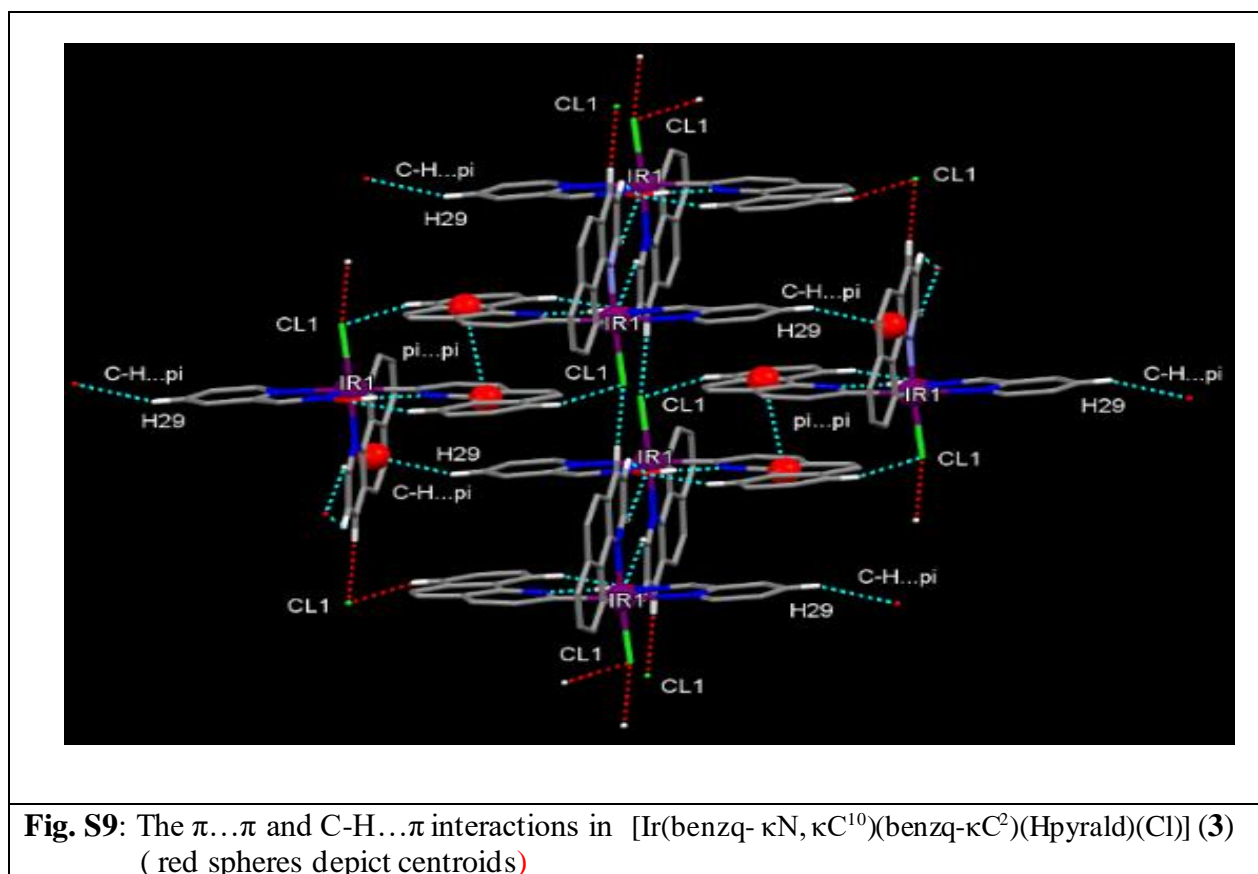
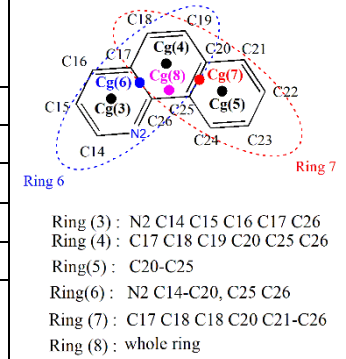


**Fig. S9:** The  $\pi \dots \pi$  and C-H... $\pi$  interactions in  $[\text{Ir}(\text{benzq}-\kappa\text{N}, \kappa\text{C}^{10})(\text{benzq}-\kappa\text{C}^2)(\text{Hpyrald})(\text{Cl})] (\mathbf{3})$  (red spheres depict centroids)

**Table: S4:** List of Intermolecular stacking parameters

Centroids	$d_{\pi-\pi}$ (Å)	Cg-Cg distance	Slippage distance (Å)	$\alpha/^\circ$	$\beta/^\circ$	$\gamma/^\circ$	
Cg7-Cg8 <sup>v</sup>	3.4895(11)	3.547(2)	0.635	1.88(14)	10.3	10.3	
Cg8-Cg5 <sup>v</sup>	3.4857(12)	3.541(3)	0.639	2.7(2)	10.4	9.9	
Cg8-Cg7 <sup>v</sup>	3.4893(11)	3.546(2)	0.633	1.88(14)	10.3	10.3	
Cg7-Cg7 <sup>v</sup>	3.5279(12)	3.624(3)	0.829	0.00(17)	13.2	13.2	
Cg6-Cg5 <sup>v</sup>	3.4768(12)	3.512(3)	0.462	3.3(2)	7.6	8.7	
Cg4-Cg5 <sup>v</sup>	3.527(1)	3.622(3)	0.868	1.8(3)	13.9	12.4	



Symmetry code: (v) 2-x, -y, 1-z ; I and J are two aromatic rings: Cg = Centroid

$d_{\pi-\pi}$ =Average perpendicular distances of Cg(J) on ring I and Cg(I) on ring J

Slippage distance = Distance between Cg(I) and perpendicular projection of Cg(J) on Ring I

$\alpha$  = Dihedral angle between the planes (I and J) of interacting rings

$\beta$  = Angle Cg(I)-Cg(J) vector and normal to plane I

$\gamma$  = Angle Cg(I)-Cg(J) vector and normal to plane J

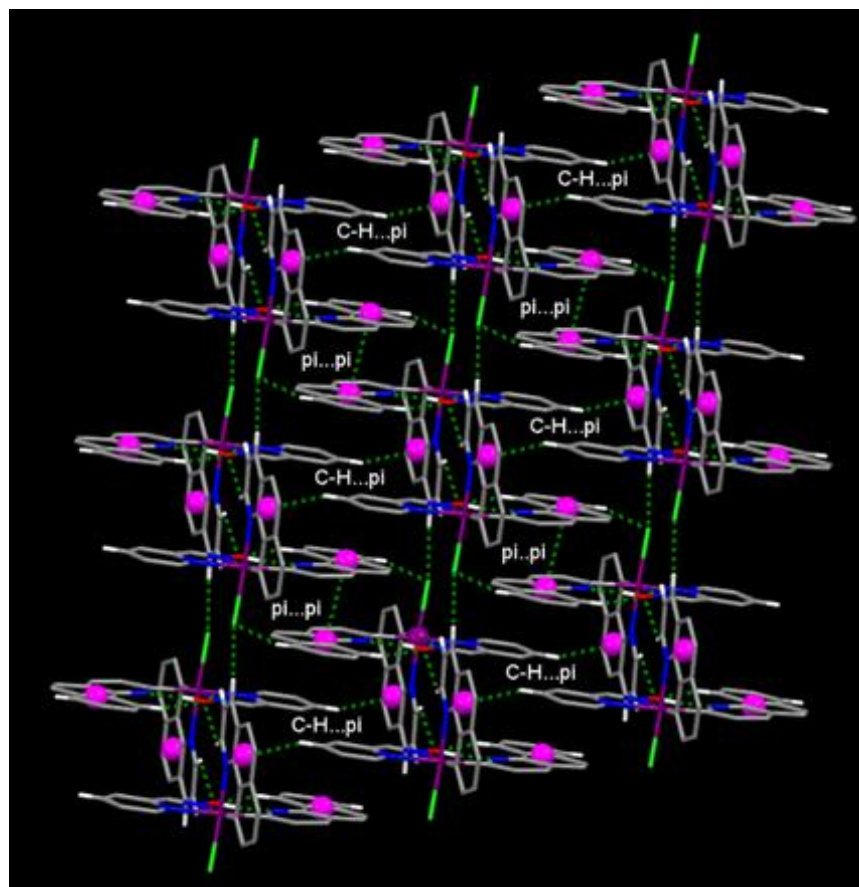


**Fig. S10:** The packing diagram of  $[\text{Ir}(\text{benzq}-\kappa\text{N}, \kappa\text{C}^{10})(\text{benzq}-\kappa\text{C}^2)\text{Hpyrald})(\text{Cl})]$  (**3**) is viewed perpendicular to (010) plane (pink spheres depicts centroids, ---- lines represent hydrogen bonding and C-H...pi interactions)

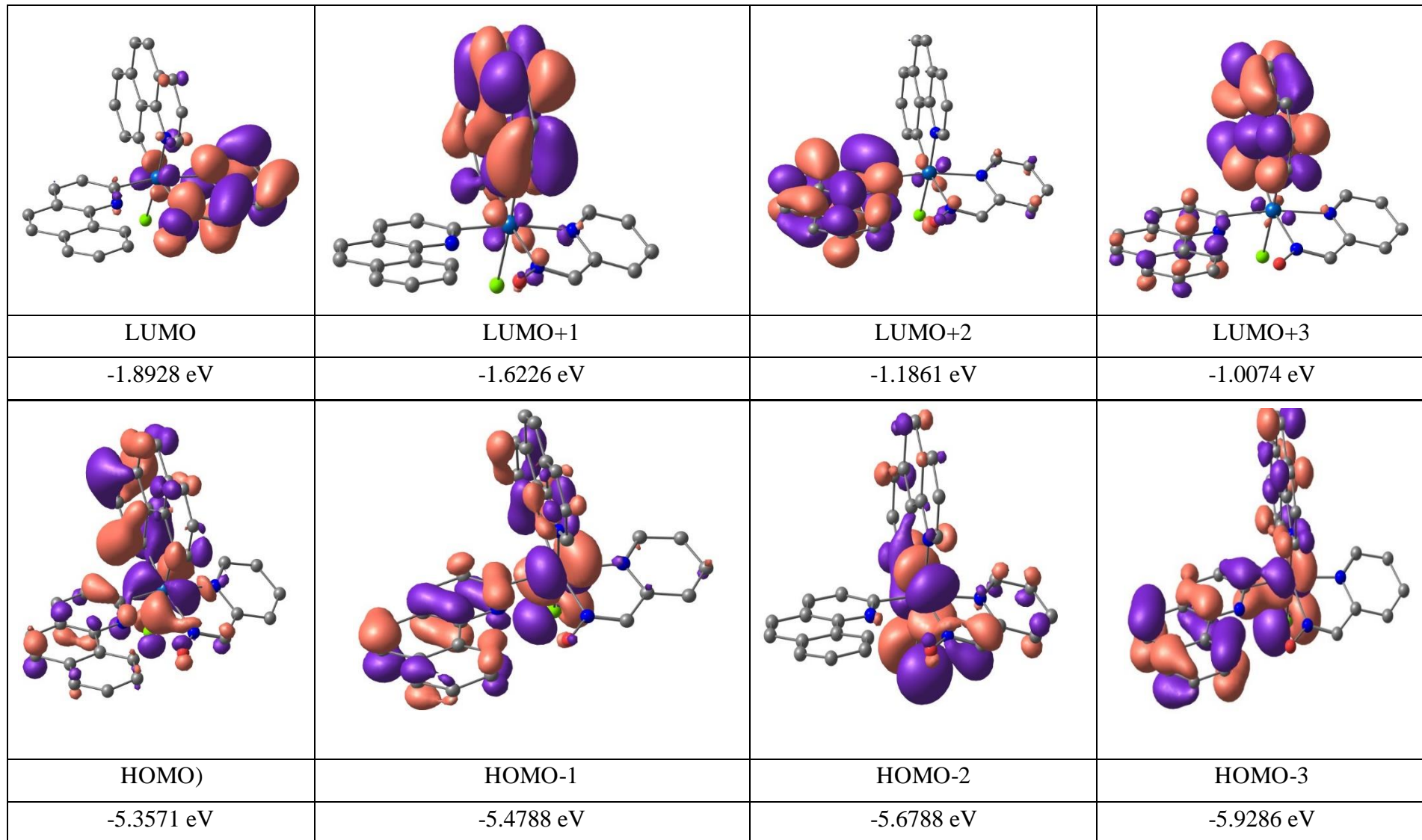


**Fig. S11.** The Kohn–Sham orbital contours (isosurface contour value = 0.03) for key orbitals of the  $[\text{Ir}(\text{benzq}-\kappa\text{N},\kappa\text{C}^{10})(\text{benzq}-\kappa\text{C}^2)(\text{Hpyrald})(\text{Cl})]$  (**3**) computed at the TD-DFT/SMD<sub>(Dichloromethane)</sub>/B3LYP-D3/def2-TZVP (Ir), 6-31G\*\* (C, H, N, O, Cl) level of theory. Hydrogens are omitted for clarity

**Table S5:** Selected TDDFT data of  $[\text{Ir}(\text{benzq}-\kappa\text{N}, \kappa\text{C}^{10})(\text{benzq}-\kappa\text{C}^2)(\text{Hpyrald})(\text{Cl})] (\mathbf{3})$ 

Complex	Nature of transition	Energy(eV)	Oscillator factor	Computed $\lambda_{\max}(\text{nm})$	Observed $\lambda_{\max}(\text{nm})$
Complex ( <b>2</b> )	HOMO→LUMO	2.7403	0.0066	452.44	<b>Not observed</b>
	HOMO-1→LUMO	2.7938	0.0134	443.78	425
	HOMO-2→LUMO	3.0443	0.0994	407.27	425
	HOMO-1→LUMO+1	3.1956	0.0325	387.98	384
	HOMO-3→LUMO+1	3.4869	0.0103	355.57	355

**Table S6:** Electronic, Emission and Electrochemical data of complex (**2**) and (**3**)

Complex	Electronic spectral data $\lambda$ (nm) ( $\epsilon \times 10^3 (\text{M}^{-1}\text{cm}^{-1})$ ) <sup>a</sup>	Phosphorescence data <sup>a</sup>	Electrochemical data <sup>b</sup> [E(V) vs SCE]
$[\text{Ir}(\text{benzq}-\kappa\text{N}, \kappa\text{C}^{10})(\text{pyrald})] (\mathbf{2})$	500(1.52) <sup>c</sup> , 428(7.68) <sup>c</sup> , 382(13.79) <sup>c</sup> , 282(49.26), 258(63.15)	539, 591	0.94 <sup>d</sup> , 1.35 <sup>d</sup> , -1.32 <sup>e</sup>
$[\text{Ir}(\text{benzq}-\kappa\text{N}, \kappa\text{C}^{10})(\text{benzq}-\kappa\text{C}^2)(\text{Hpyrald})(\text{Cl})] (\mathbf{3})$	500(0.94) <sup>c</sup> , 425(6.35) <sup>c</sup> , 384(12.09) <sup>c</sup> , 355(16.35) <sup>c</sup> , 282(52.32)	594, 641	1.27 <sup>d</sup> , 1.59 <sup>d</sup> , -1.41 <sup>e</sup> [1.06V, -1.14 (Hpyrald)] <sup>f</sup>

<sup>a</sup>=dichloromethane solution<sup>b</sup> = in acetonitrile solution<sup>c</sup> = shoulder<sup>d</sup> =  $E_a$  values<sup>e</sup> =  $E_c$  values<sup>f</sup> =  $E_a$  and  $E_c$  values of pyridine-2-aldoxime

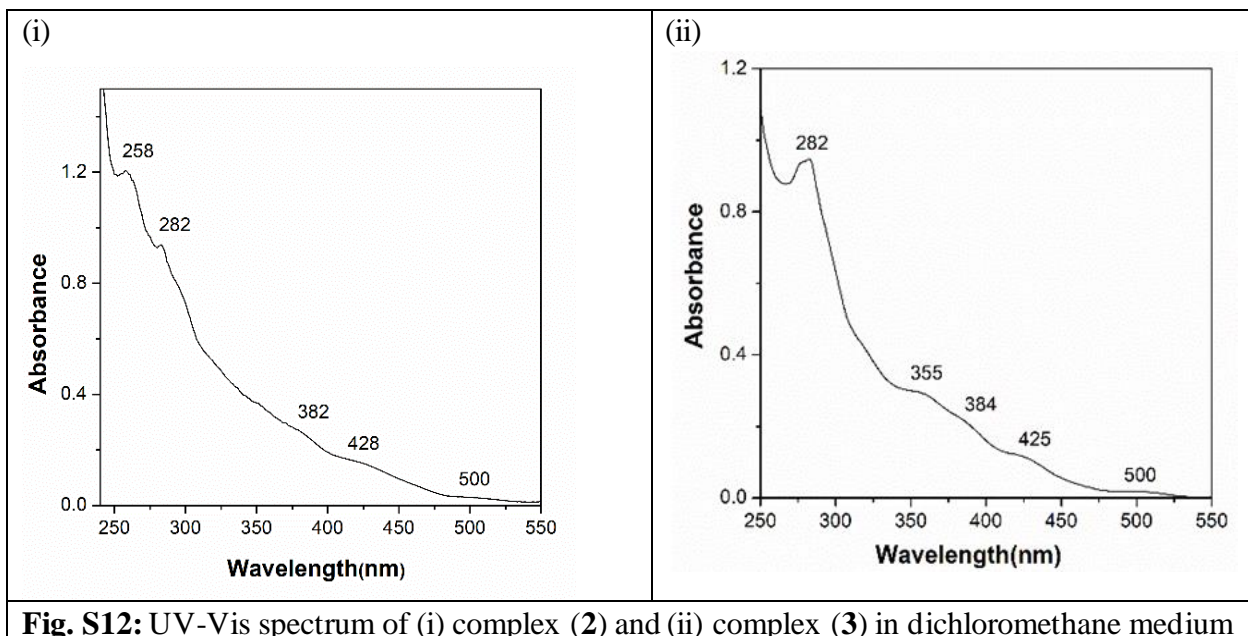


**Fig. S12:** UV-Vis spectrum of (i) complex (2) and (ii) complex (3) in dichloromethane medium

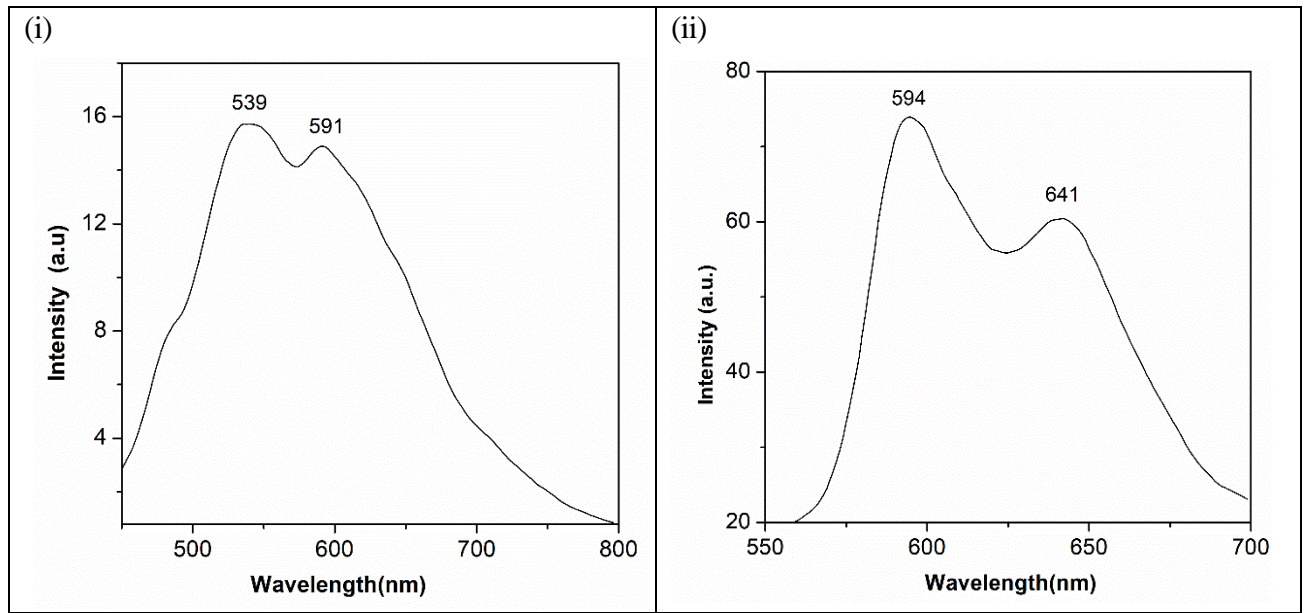


**Fig. S13:** Emission spectrum of (i) complex (2) and (ii) complex (3) in dichloromethane medium

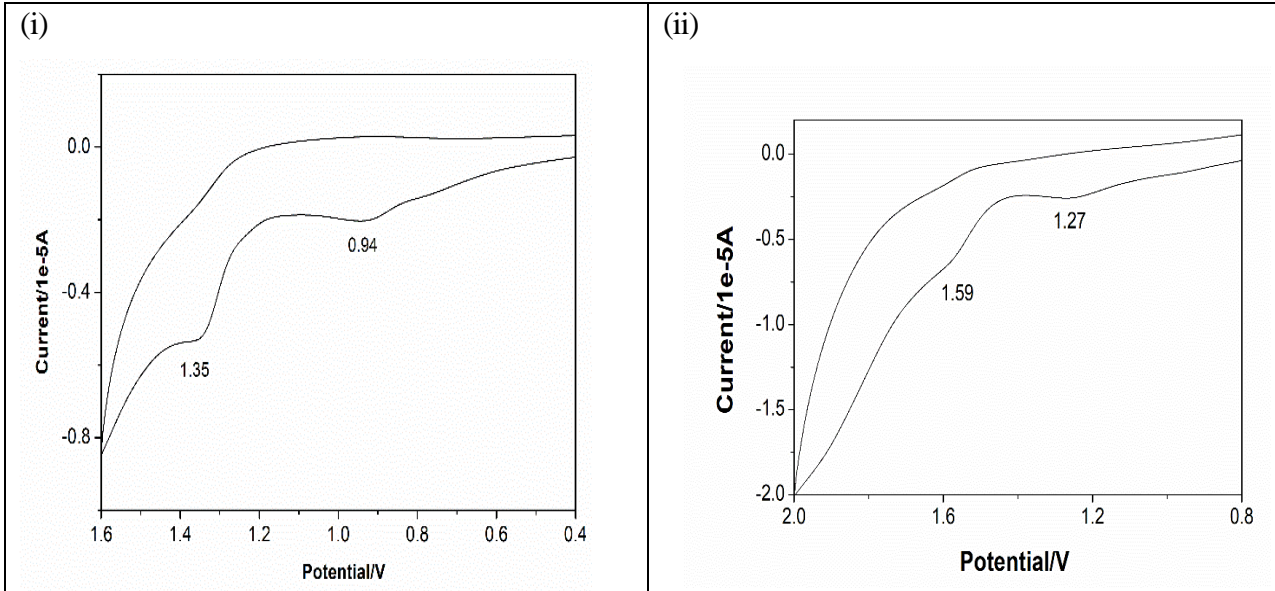


**Fig. S14:** Cyclic voltammogram of (i) complex (2) and (ii) complex (3) in acetonitrile solution